Review and simulation of the electrochemical response of cobalt hydroxide electrodes for energy storage

Gabriel Garcia Carvalho

gabriel.carvalho@tecnico.ulisboa.pt

Instituto Superior Técnico, Universidade de Lisboa, Portugal

21 January 2021

Abstract – The pseudocapacitive mechanisms related to cobalt hydroxide nanofoams have been studied within the scope of supercapacitors' use for energy storage. A comprehensive review has been conducted highlighting the positioning and evolution of electrochemical systems, focusing in the materials and major working principles of devices such as dielectric capacitors, electrolytic capacitors, and supercapacitors (under which EDLCs and pseudocapacitors are included). To further understand the application and functionalization of cobalt hydroxide nanofoams, a review about 3D electrode architectures was made, exposing the most important parameters and operating conditions related to the purpose, synthesis and use of these nanostructures. Additionally, a computational MATLAB simulation was developed towards understanding the mathematical theoretical models present in literature that best define the electrochemical response of pseudocapacitive materials, further promoting the knowledge about pseudocapacitors and their placement in the electrochemical energy storage field.

Keywords **–** Nanofoam, cobalt hydroxide, DHBT electrodeposition, supercapacitor, pseudocapacitor, cyclic voltammetry, energy storage

I. INTRODUCTION

The need of energy storage

World population has been growing every year as economic growth and better life standards continue to increase. Energy demand presses the world towards smarter cities and efficient energy supply systems which steadily face greener and more renewable alternatives rather than the conventional fossil counterparts. With the exciting potential and increasing domination of renewable energy sources, the management of the available produced energy becomes a greater challenge due to their intermittent nature, thus limiting the scope of their use. Once answered by storing wood logs and now by storing electrons, this challenge can only be addressed with highly efficient storage systems that prevent needless wastes of energy while opening the door to a wider array of future applications.

According to the International Energy Agency (IEA), energy consumers are increasingly investing in systems deployed closer to them and within their higher control which allows for a better management of the energy at a much faster rate than the rate at which the grid-scale deployment is evolving [(1)]. This worldwide capacity growth is due to the ongoing investment in renewables with decreasing costs of operation and deployment, posing not only a considerably more sustainable option but also a cheaper and cleaner alternative to the use of fossil fuels [(2,3)].

Energy storage methods

Energy storage systems are categorized in mechanical, thermal, electrical, chemical, and electrochemical. Each method stores energy under different principles and is applied in different scenarios according to their operating conditions.

Mechanical energy storage takes advantage of the kinetic and potential energy of solids and fluids to use the physical forces applied to them (like gravity or decompression) as basic working principles of charge and discharge. Hydropower is a prime example of the scale that mechanical systems can successfully reach, making up 96,2 % of the worldwide energy storage capacity [(4)]. Thermal energy storage stores energy in the form of heat, making use of the heat transfer phenomena to store and release the heat when necessary. This energy can take the form of sensible heat (changes in temperature, and thus, in the energy state) or latent heat (phase transformations that involve greater amounts of heat transfer at constant temperature). These are ingenious systems used in house ambient and district heating and cooling applications (DHC) that go as far as supplying energy to entire villages and cities. Electrical systems store energy in the form of electricity by manipulating the flow of charged particles in ionic/dielectric fluids between the electrodes of a capacitor or through magnetic shifts in superconducting magnets. Due to the inherently low energy capacity of these electrical devices their applications usually extend to small-scale dimensions and are accompanied with other energy storage devices with higher energy density. Chemical energy storage systems store energy with endothermic reactions and discharge the respective energy with reversible exothermic reactions. In the great majority of cases, this charge/discharge system translates in the dissociation of a chemical compound followed by its respective synthesis. Electrochemical energy storage systems, just like the name indicates, combine electrical and chemical processes that involve electrochemical reactions with electron transfer through conducting electrodes to store the energy. Unlike capacitors, electrochemical systems require an electrolyte and rely on redox reactions occurring at the bulk, or surface, of an electrode. These devices include batteries, ultra-batteries, and redox-based supercapacitors. It is extremely relevant for this work to fully understand the

functioning of batteries and redox supercapacitors in order to acknowledge the advantages and disadvantages of each when it comes to develop highly versatile, powerful, and energetic electrochemical devices.

Electrochemical capacitors

Electrochemical capacitors (ECs), otherwise known as supercapacitors or ultracapacitors, are the strategic establishment of a complementary response between high-energy (batteries) and high-power (capacitors) density devices. Neither batteries or capacitors are able to provide simultaneously large yields of energy while maintaining fast rates of charge and discharge. This raised the interest in different device assemblies included in the ECs family: the redox supercapacitor, the pseudocapacitors, the electrochemical double layer supercapacitors (EDLCs), and the hybrid devices. Conventional batteries can reach energy capacities around 100 Wh/kg, greatly surpassing conventional capacitors, but display much lower power density. Batteries are typically used to store high quantities of energy while capacitors fill the needs in terms of power requirements. Therefore, these two classes of devices are specialized in complementary applications where either energy or power densities are of utmost importance. Nevertheless, a gap is left in the array of electrochemical applications as the two referenced extremes dominate the electrochemical energy storage field. This gap opens several investigation opportunities to create solutions between the battery and conventional capacitors (Fig. 1).

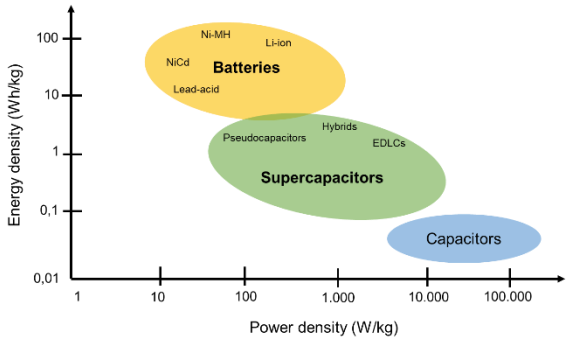

Fig. 1 - Energy/power densities of electrochemical devices

These solutions include the redox and the pseudo supercapacitors and hybrid devices (combine a battery type electrode with a supercapacitor type electrode) that can potentially translate into more versatile systems with increased energy density while providing good power capacity.

Work objectives

The intention of this work is to deliver an extensive state of the art about supercapacitors to further improve the theoretical and practical knowledge for electrochemical energy storage. Furthermore, special focus is given to the production and functionalization of pseudocapacitive nanofoam structures made of cobalt hydroxide. The work intends to better comprehend the routes for production of these materials and the mechanisms governing their electrochemical response, by reviewing the current literature and conducting computational simulations (with MATLAB software) to predict the electrochemical response of the cobalt hydroxide system.

II. STATE OF THE ART

Dielectric capacitors

The most conventional and simple capacitors are the dielectric capacitors which are often named according to the dielectric they are composed of (e.g. vacuum, glass, ceramic, and film capacitors). The assembly of dielectric capacitors consists of two metal electrodes (i.e. polarized or non-polarized, depending on the application) with surfaces opposite to each other, pressing the dielectric material between them (Fig. 2). The electrodes are connected externally by a circuit that provides the energy during charge and receives the stored energy throughout discharge, when the process is reversed.

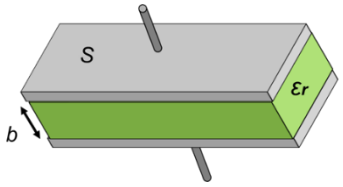

Fig. 2 - Dielectric capacitor

The dielectric is a material with polarizable molecules that face the charged electrodes with respective opposite charges. It is crucial for the dielectric to be an efficient insulator so no current flows through the media, staying stored electrostatically in the electrode's surface [(5)]. Where the electrostatic charge storage lacks in energy density gains in power capacity. These devices are able to charge and discharge at very high rates (a few milliseconds) sustaining power densities around 1 to 10 kW/kg, incredibly higher than conventional batteries. The total stored electric charge of a capacitor can be calculated using equation [1] that proportionally relates the stored energy and the potential window of the system with the capacitance of the device. The devices capacitance can be calculated with equation [2].

$$\Delta Q = C.\Delta\psi \qquad [1]$$

$$C = \varepsilon_0.\varepsilon_r.S/\,b \qquad [2]$$

ΔQ is the stored charge (coulombs, C), C is the capacitance (farad, F), $\Delta\psi$ is the potential window (volt, V), ε_0 and ε_r are the electrical relative permittivity of vacuum, and of the dielectric material, respectively. S is the surface area of the electrode plates and b the thickness of the dielectric material. Therefore, a good dielectric capacitor has a dielectric media with high permittivity, a good response to the polarization effect, a very thin thickness, and a big surface area.

Electrolytic capacitors

Electrolytic capacitors store electrostatic charge just like dielectric capacitors. The fundamental working principle of these devices is that a metal electrode can be anodized to create thin films of metal oxide at its surface which isolate the electrode. This process is the effective passivation of the metallic material which can be obtained by submitting the electrode to a very specific potential that allows the formation of oxygen in the anode and hydrogen in the cathode, thus, enabling the synthesis of a metal oxide adjacent to the electrode surface. The name of this capacitor results from the great similarity of the device's layout to one of an electrolytic

cell, where an electrolyte is pressed in the middle of two polarized electrodes. The anodization process begins by submitting the target electrode to a very specific voltage that favours oxidation reactions at the positive electrode (anode oxidation - anodization) and reduction in the negative electrode, thereby defined as cathode. While hydrogen builds up at the cathode (I), the metal of the anode is oxidized (II).

$$2H^+ + 2e^- \rightarrow H_2 \qquad \text{(I)}$$

$$M + nH_2O \rightarrow MO_n + n2H^+ + n2e^- \qquad \text{(II)}$$

M is the exposed metal material of the electrode and n the stoichiometric number of water molecules necessary for the anodization to proceed. A prime example of an anodization process is the formation of anodic aluminium oxides (AAO). The anodization process is often referred to as passivation due to the non-reactive properties of the resulting oxides. What ultimately sets passivation differently from a corrosion process (also enabled by metal oxidation) is the potential and alkalinity conditions upon which the oxidation occurs. These conditions can be studied by a Pourbaix diagram of the respective system. Among the most studied materials is aluminium [6-8], magnesium [9-11], niobium [12-14], and titanium [15-17]. The applications and focus of these investigations range from metal coating for biomedical applications, corrosion protection, synthesis of porous films, metal self-colouring, and, evidently, energy storage.

Electrochemical double-layer capacitors

Named after the double-layer effect first described by Helmholtz, electrochemical double-layer capacitors (EDLCs) are a type of supercapacitor that store electrostatic energy through the reversible adsorption of electrolyte ions at the surface of the electrode. EDLCs differ from conventional capacitors due to the local polarization of the electrolyte's ions and the consequent formation of the double-layer planes [18]. The double-layer is a complex molecular phenomenon that several different models have attempted to describe by understanding the behaviour of the electrolyte's components and their realistic interactions with the electrode's surface. The development of these models is a continuation of the conclusions of the first theories concerning the double-layer, attempting to answer the present flaws and deviations from reality the best way possible by formulating new assumptions and considerations regarding the properties of the electrolyte's components. The classical theories that will now be explained are present in Fig. 3.

Helmholtz developed the understanding that ions of the opposite charge of electrode's polarity simply neutralize the counter charge at a distance d which is the distance from the ion's centre to the surface of the electrode. The layer defined by d, in Fig. 3a, is classically named as the *Helmholtz layer* which separates solid phase (electrode) from the electrolyte's bulk. The separation of charges that results from the ion neutralization represents a local case of dielectric capacitance as charge is stored electrostatically within the Helmholtz layer. This created a potential gradient between the electrode's surface and the ions, ψ_0 being the electrode's potential and ψ the potential across the Helmholtz layer. Therefore, equation [2] can be applied to quantify the layer's capacitance. This compact counter-ion model is considered to be rigid as it does not accurately describe the reality of the double-layer, disregarding the effects of other components in the electrolyte's diffuse layer and the existence of adsorption processes in the surface of the charged conductor. It is also important to refer that the ions are in a solvent-rich phase that should be pertinently considered in order to optimize the double-layer model as the presence of solvent molecules should increasingly affect the thickness of the Helmholtz layer, and, consequently, the layer's capacitance. The Helmholtz model is thereby a highly simplistic theory that was set as a primary approach towards the complex phenomena that is the double-layer.

Gouy and Chapman state that the potential between the electrode's surface and the ion's counter-charge is not entirely accurate with the dielectric capacitor model, admitted by Helmholtz, but rather in line with the diffusion of the solvated ions that diffuse towards the electrode surface. While the model (Fig. 3b) admits that the electrode charge is neutralized with ions of the opposite charge, it also suggests that the counterions, present within the diffuse layer (name hereby given to the double-layer), diffuse through the electrolyte according to their kinetic energy, setting the double-layer thickness through an assumed Boltzmann distribution. According to literature [19] this model deviates from reality when applied to cases with highly charged double-layers where the thickness of the layers is greater than the thickness calculated, revealing a fundamental limitation in the Gouy-Chapman model.

Another limitation in the Gouy-Chapman model is that it does not consider the size of the ions as a resisting factor in their approach towards the surface of the electrode. It approximates every component as point charges [19] only limited by their kinetic energy during diffusion. Stern's modification (Fig. 3c) of this model states that the Helmholtz

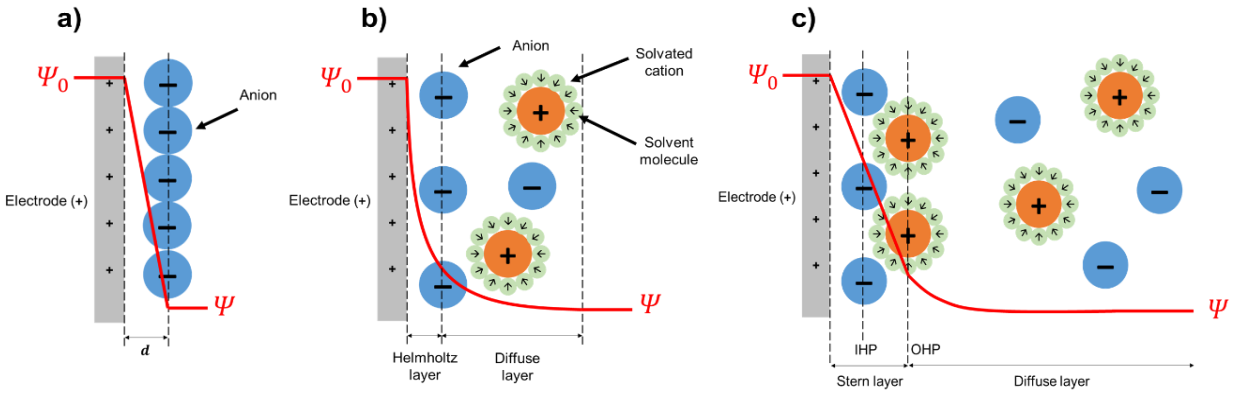

Fig. 3 – Classical models of EDL a) Helmholtz, b) Gouy-Chapman, c) Gouy-Chapman-Stern

notion of a primary layer is incomplete, and that Gouy-Chapman diffuse layer does not apply as close to the surface as it's claimed by the previous theory. This model thereby assumes the existence of specific adsorption of ions between the immediate counterions in the charged electrode, explaining that between the counterions and the diffuse layer rests two planes defined by the opposite charged ions. Taking the example of a positively charged electrode, this model theorizes that the negative ions that neutralize (specific adsorption) the electrode's charge define the inner Helmholtz plane (IHP) while the non-specifically adsorbed solvated ions define the outer Helmholtz plane (OHP). The distance from the electrode surface to the OHP is named as the *Stern layer* and sets a much more realistic dielectric-like behaviour before the diffuse layer of Gouy-Chapman model is defined. Gouy-Chapman-Stern model answers the limitation of the unreliability of the previous theory regarding highly charged double-layers as it further pushes the boundary of the diffuse layer away from the surface of the electrode by combining the two previously presented models into one. Note that the distance from the electrode surface to the IHP is the Helmholtz layer.

Electrode carbon-based materials

Carbon-based materials are the prime material to assemble EDLC electrodes. They are inexpensive products with very high specific surface areas (from 1000 to 3000 m2/g) resulting in highly capacitive electrochemical responses. As carbon is a highly versatile material and easy to manipulate, several different nanostructures can be synthesized with this element as well as further treatments and activation methods that transform carbon structures into more electrochemically enabling materials like activated carbon (AC), carbide derived carbons (CDC), carbon nanotubes (CNT) and graphene.

ACs are amorphous carbons of very high surface area. They are synthesized through physical and/or chemical methods that convert natural precursors (e.g. grapefruit, rice husk, straw, aloe vera, fruit skins, eucalyptus-bark, soya) into elementary carbon powders with interesting properties that are considerably appealing for electrochemical and catalytic engineering applications. The production of ACs is referred to as an accessible and simple synthesis procedure of rewarding outcome which is self-evident in the fact that activated carbons are the most used choice in EDLC electrodes despite the existence of better performing carbon-based materials. The synthesis of ACs usually comprises a carbonization step followed by an oxidizing treatment.

CDCs are created by removing metals from a carbide's lattice through thermal and chemical extractions. The most used carbide precursors are usually composed of tungsten, zirconium, silicon, and titanium. When combined with carbon, these metals (and semi-metals) form interesting lattice conformations which allow different porous structures to be created from carbides [(20)]. The metal extraction can vary in depth as the transformation process is able to define the intended percentage of removed metal, from the carbon framework. This allows an accurate tune of functional groups at the structure's surface for improved electrochemical behaviour [(21)]. Usually, the processes that convert carbides into carbons consist of chemical treatments with halogens (e.g. chlorination) and physical treatments under vacuum (e.g. vacuum decomposition).

Carbon nanotubes are another creative set of materials that illustrates how the transformation of simpler carbon-based precursors, like hydrocarbons, can result in complex and peculiar nanostructures. CNTs are hollowed carbon nanocylinders structured perpendicularly to a metal conductor, giving rise to a valuable accessible surface area with high conductivity. They are usually classified by the layer density of the nanotubes: single-wall CNTs (SWCNTs) and multi-wall CNTs (MWCNTs). Due to the preparation of CNTs being highly dependent on the growth control of carbon's crystalline order, the purity of the carbon directly influences the morphology of the synthesized nanotubes and consequently affects the specific capacitance of electrodes. The well-ordered structures allow the conjugation of CNTs with other materials that increase the energy density of the system.

Graphene is a pure carbon structure where each carbon bonds with three other carbon atoms, creating a hexagonal mesh monolayer. Graphene has the record of being both the thinnest and strongest material ever measured in materials science [(22)]. These two properties of graphene gave inherent value and research interest to this carbon-based material. Being a monolayer of atomic thickness (diameter of a carbon atom), graphene properties are very pertinent in electrochemistry. Moreover, its high thermal and electric conductivity, great high surface area (~2630 m^2/g, close to the usual ranges of activated carbon), and the ability for its 2D conformation favours to be manipulated into other carbon nanostructures. The preparation of graphene is a very delicate process. Any unwanted stacking of graphene sheets results in the irreversible formation of graphite: a bulk material composed of several bonded graphene layers that lacks the wanted and targeted properties of the isolated monolayer of graphene. Synthesis methods of graphene can be physical (mechanical exfoliation) or chemical (chemical vapor deposition, CDV) the latter one being significantly more used for graphene mass-production.

Comparing carbon-based materials is not a straight-forward task. Each one of these electrodes differ in shape, synthesis pathways, and influencing factors in the electrochemical response of supercapacitors. But the true challenge of rating these materials lies in the ingenious, and, ultimately, almost infinite ways that carbon electrodes can be optimized by simple associations with other compounds, and sometimes, with other forms of carbon (e.g. graphene-CNT electrodes). González et al. [(19)] provided an review of carbon-based electrodes and reported the most interesting values achieved by several studies.

Pseudocapacitors

Unlike EDLCs, pseudocapacitors are faradaic devices that store energy via highly reversible and fast redox based reaction mechanisms that contribute to higher energy density without greatly compromising fast charge/discharge rates. It is important to make the convenient distinction between faradaic and non-faradaic processes. These two concepts derive from the validity of Faraday's laws of electrolysis in the interface between an electrode and an adjacent electrolyte phase, labelling the behaviour and movement of charge and chemical components involved in the energy storage process. Faraday's laws state that the composition of a material in the electrode-electrolyte interface is directly proportional to the amount of electricity passed. Despite the simple mathematical definition, labelling a process as faradaic may not be as straightforward as expected. Biesheuvel and Dykstra [(23)] analysed the factors that differentiate faradaic

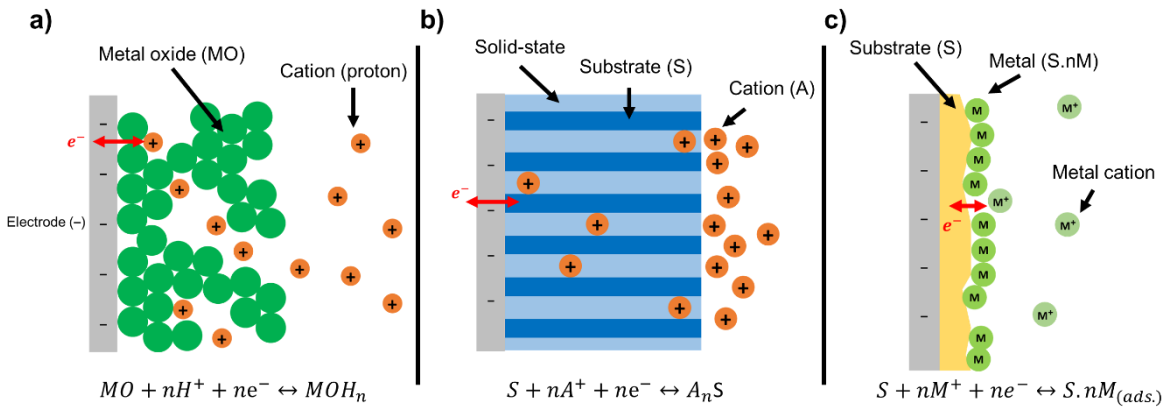

Fig. 4 - Pseudocapacitive mechanisms: a) redox, b) intercalation, c) underpotential deposition

from non-faradaic processes by considering the presence of the movement of charged species, and the location of the electrode-electrolyte interface. It is a long and profound discussion that goes beyond the objective aimed in this work. Therefore, it is hereby assumed that a faradaic process is one where any redox reaction occurs at the electrode-electrolyte interface. By opposition, a non-faradaic process is one that separation of charge (electrons in electrode side and cations in Helmholtz layer) in the electrode-electrolyte interface occurs as a result of the EDL phenomena (electrostatic storage).

Pseudocapacitance is the term that refers to the faradaic processes encompassed by this charge storage system. Depending on the electrode material's properties, pseudocapacitance can be expressed as inherently intrinsic or extrinsic. Intrinsic pseudocapacitance is exhibited in a broad spectrum of morphologic conditions showcasing the same electrochemical pseudocapacitive behaviour regardless of the structure of the material. Extrinsic pseudocapacitance, contrary to the intrinsic one, manifests itself differently with the morphology of the active material as its behaviour is not the same in crystal conditions as it is in layered/porous structures. It is important to understand whether the pseudocapacitive behaviour of a material is intrinsic or extrinsic in order to efficiently optimize the electrochemical response to the intended goal values. There are three known mechanisms that create different pseudocapacitance behaviours: fast reversible redox reactions (Fig. 4a), intercalation processes (Fig. 4b), and underpotential deposition (Fig. 4c).

What characterizes pseudocapacitors the most is their redox-like feature responsible for the high energy capacity at fast rechargeable rates. Faradaic processes in pseudocapacitors consist of surface, or near-surface, fast reversible redox reactions. With these reactions occurring at the surface, the SSA is one of the most important factors liable to the optimization of the electrochemical response. This is where the creative combination of pseudocapacitive materials (e.g. metal oxides) with interesting 3D nanostructures takes place. The charge redox mechanism of pseudocapacitors is very similar to the one of batteries. During the charge process, an external power supply injects electrons in the circuit forcing the current to flow from the positive to the negative electrode. The electronic density in the negative electrode attracts the cations from the electrolyte to be reduced in the electrode's active material. The most used and studied pseudocapacitive materials are transition metal oxides (TMOs) which participate in the redox reactions by reacting with the electrolyte's protons (III) or eventually other ions.

$$MO + nH^+ + ne^- \leftrightarrow MOH_n \qquad (III)$$

MO being the metal oxide and MOH_n its reduced form. During the discharge process, the inverse reaction occurs as the electrode surface is oxidized, releasing protons to the electrolyte solution while electrons are transferred to the external circuit. The process of opposite polarization exists as well with OH^- in solution instead of protons.

Intercalation pseudocapacitance is the insertion of ions (e.g. Li^+, Na^+, H^+) through layered nanostructures of an electrode. These ions react and provide an electron transfer across a solid-state interface within the active material. It is a case of a redox reaction occurring through a solid-state diffusion. During discharge, the opposite process occurs where the de-intercalation of the ions takes place after receiving the transferred electrons from the collector. This process requires a well-defined two-dimensional layered structure and large inter-layer spacing in order to enable the intercalation of ions within the active material [24]. Furthermore, intercalation pseudocapacitance allows the faradaic process to occur without phase changes in the crystalline structure of the material which prolongs its cycling life at fast charge/discharge rates, and, consequently, lowers its rates of degradation [25].

In underpotential deposition (UPD), the metal onto which the deposition occurs, the substrate, serves as an inert support for interesting active materials. Underpotential deposition translates into a highly promising method for substrate coating that allows the manipulation of substrate morphology without needing the direct synthesis of 3D structures of the active material itself, not only saving the quantity of active material needed for the system but also allowing the creation of other structures that might have not been initially possible with the active material alone. The study of UPD is mostly aimed towards the functionalization of electrode surfaces and optimizing the least quantity needed of a certain active material for the electrochemical behaviour to occur, rather than focusing on its role in pseudocapacitive energy storage.

Electrode materials research can be divided between the study of nanostructures and composites. Optimizing nanostructures involves the improvement of morphological parameters such as surface area, active sites, and diffusion pathways that highly influence the ions' behaviour in relation to the electrode material, whereas in composites, the research aims at the optimization of electrical conductivity and structural stability [26].

MOHs are materials of high specific capacitance and

electrical conductivity. A wide variety of these metals has been studied in the past decade, the most well-known metals used in electrodes being Ru, Ir, Mn, Ni, Co, Sn, V and Mo [19]. The evaluation of MOHs intrinsic pseudocapacitance cannot be complete if the metal costs are not taken into consideration. The high capacitance observed in metal oxides (MOs) is a consequence of the multiple oxidation states that these metals exhibit during proton exchange, which, alongside the fact these redox processes occur in the surface and/or near-surface electrode regions, greatly facilitates ion adsorption [18]. A review has been made in this work dedicated to the comparison of multiple capacitance studies of ruthenium, cobalt, and nickel oxide electrodes with the objective of providing a more new and diverse insight of latest articles. The reviewed literature logically suggests that cobalt and nickel oxides clearly surpass ruthenium oxide capacitance under most conditions. In fact, the best ruthenium oxide result [27] (1469 F/g) is an interesting combination with cobalt which is approximately >100% greater than RuO_2 in its solo electrode oxide form. Therefore, it is hereby suggested that nickel and cobalt oxides are promising options among the known MOs previously mentioned. Nevertheless, it is to be noted that the ultimate choice of which MOHs electrodes should be used is considerably dependent of the operating conditions that the device is intended to be submitted to, as different redox materials exhibit changes of oxidation states at different voltage windows [28].

Nickel hydroxide, $Ni(OH)_2$, manages to exhibit a greater theoretical capacitance of 3650 F/g, considerably surpassing its oxide counterpart, NiO_x (~2500 F/g). The amazing specific capacitance of $Ni(OH)_2$ is believed to be deeply related to its loosely crystalline structure, assisting in the intercalation of ions during the charge/discharge process which consequently results in a greater electrochemical performance [26]. The behaviour of cobalt hydroxide, $Co(OH)_2$, is practically analogous to its nickel counterpart. The two elements are usually seen as electrochemical twins, with similar layered hexagonal nanostructures that are often combined in literature [29-32] for improved responses. The energy storage mechanisms of Ni and Co hydroxides are not entirely understood yet, but Shi et al. exposed two interesting theories concerning the species involved in the change of oxidation states of Ni hydroxide electrodes [26]. Both are accepted and studied in literature, but special attention should be given to the ones that involve hydroxides as reactants and products of the charge storage, given that the spontaneous formation of $Ni(OH)_2$ occurs by combination of water and hydroxyl molecules with NiO [33]. Furthermore, the $Ni(OH)_2$/NiOOH redox pair is known to establish a multi-phase system that further clarifies the processes happening during the aging and overcharge of a Ni hydroxide electrode, as well as explaining which phases contribute to better specific capacitance (α-$Ni(OH)_2$/γ-NiOOH).

III. METAL NANOFOAMS

It has been widely reported that devices with simple 2D structures result in considerable difficulty in reaching the targeted high performances. Researchers' initial answer to this challenge was synthesising ultra-thin active materials onto the current collectors, which allowed an easier and efficient charge storage. However, the commercial reality of these devices requires a higher mass load than the electrode investigation field usually takes into consideration. Sun et al. [34] have made an interesting review concerning the evolution of electrode's architecture. The way science addressed this challenge was with the creation of 3D nanostructures which allows access to active sites present within the bulk of the electrode. The development of 3D architectures can vary incredibly depending on the chemical building blocks that are used to synthesize the nanostructures with enough SSA that allows a much more efficient performance of the device. Metal foams are known to have a higher electrical conductivity than carbon-based 3D structures as well as the easier manipulation of their morphology [35].

Synthesis by electrodeposition

This process is practically identical to the underpotential deposition covered in the previous chapter with the exception that electrodeposition occurs at an overpotential voltage, which, in contrast, allows the deposition of several layers of metal ions onto the substrate. Some nanostructures, such as nanofoams, are synthesized by electrodeposition with high SSA as a result of the series of reactions between metal ions and hydrogen molecules that compete at the electrode's surface. As the solubilized metals deposit onto the substrate, adsorbed hydrogen in its surface (IV) reacts with the protons in solution to form H_2 (V) which will desorb from the metal substrate and diffuse through the metal ions as their deposition occurs simultaneously (VI). Reactions (IV) to (VI) contribute to the production of H_2 and the process they define is referred to as *H_2 evolution*, crucial to the formation of highly porous metal nanostructures by utilizing the formation of H_2 at the substrate surface and its following desorption to the solution's bulk as a pathway creator of nanoscale spaces within the depositing metal atoms.

$$H^+_{(aq)} + e^- \rightarrow H_{(ads)} \quad \text{(IV)}$$

$$2H_{(ads)} \rightarrow H_2 \quad \text{(V)}$$

$$M^{n+}_{(aq)} + ne^- \rightarrow M_{(s)} \quad \text{(VI)}$$

The production of metal nanofoams by electrosorption is known as dynamic hydrogen bubble template (DHBT). The diffusion of H_2 bubbles creates tunnels that grow from the substrate surface to the bulk of the solution, forcing a porous framework of the deposited metal. Arévalo-Cid et al. [36] experimentally showed the influence of electrodeposition duration in the pore sizes of cobalt nanofoams, suggesting that consecutive layers of cobalt are built with increasing pore size overtime. The increasing pore size suggests that the H_2 bubbles increase in size as well, which Arévalo-Cid et al. thereby concludes that this phenomena is a consequence of coalescing hydrogen bubbles within the metal deposit, resulting in a continuously increasing bubble size as H_2 diffuses farther away from the metal substrate (Fig. 5).

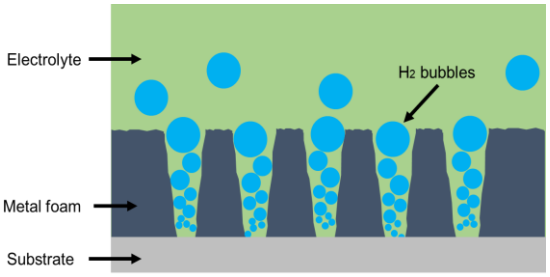

Fig. 5 - Influence of H_2 coalescence in DHBT electrodeposition

Functionalization treatments can result in different electrochemical responses depending on its duration and degree, as shown by the work of Naureen of thermal and

oxidative activation of cobalt nanofoams [37].

IV. CV SIMULATION

Computational simulations of cyclic voltammetry were developed in order to observe the current and voltage values as well as the shape of the CV curves and draw conclusions regarding the behaviour of the system. The current work will attempt to simulate the case of energy storage in a cobalt hydroxide electrode. In CV, current is measured across a potential sweep which covers a forward and backward stage across a well-defined voltage window that depends on the nature of the electrode active material. The mathematical relationships between the current and voltage are not straightforwardly obtained. Other variables such as electrolyte concentration, electron-transfer rate, time, and distance to the electrode's surface are among the main parameters that vary when conducting a CV. The potential sweep varies linearly with time under a specific scan rate (ν) in Vs^{-1}. The minimum and maximum potential, ψ_{min} and ψ_{max}, define the potential window ($\Delta\psi$) and the shape of a potential sweep can be observed by plotting potential in function of time (Fig. 6).

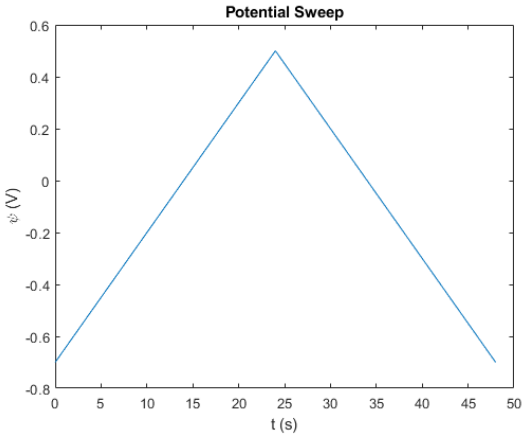

Fig. 6 - Potential sweep at scan rate of 50 mV/s

With the potential defined, kinetic and diffusion models were then discretized and applied based on the Butler-Volmer kinetics and Fick's 2nd law of diffusion.

$$j_F = j_0 \left[exp\ exp\ \left(\frac{\alpha n F \eta}{RT}\right) - exp\ exp\ \left(\frac{-(1-\alpha) n F \eta}{RT}\right) \right] \quad [3]$$

$$\frac{\partial}{\partial t} = D_i \frac{\partial^2 C_i}{\partial x^2} \quad [4]$$

Where j_F and j_0 are the faradaic current density and the exchange current density (A/m^2), respectively, α the system's transfer coefficient, n the number of transferred electrons, R the gas law constant (J/K mol), T the temperature (K), η the overpotential (V), D_i the diffusion coefficient of the electroactive specie i, C_i its concentration (mol/cm^3), and x the distance to the electrode (cm). The diffusion gradients were solved with the finite point-system method as described by Brown [38]. The obtained CV curve simulation is displayed in Fig. 7.

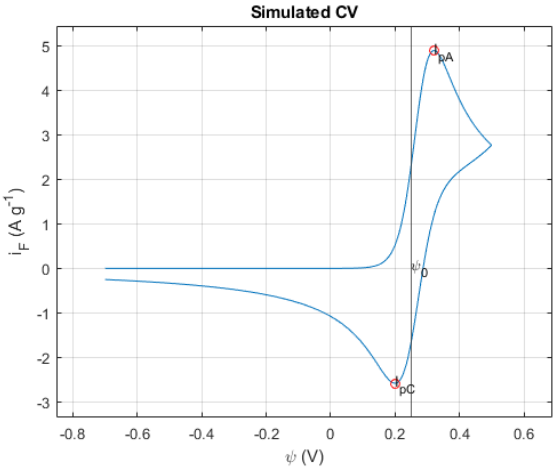

Fig. 7 - Simulated CV curve for the cobalt hydroxide system

It is immediately observed two well defined peaks in the obtained CV curve, classic indication of the faradaic behaviour of the system. In Fig. 7, the anodic and cathodic current peaks are highlighted by i_{pA} and i_{pC}, respectively defining the oxidation and reduction reactions. According to the simulated CV curve, the electrochemical response starts, as intended, from the minimum/starting potential (ψ_{min}) of - 0,7 V from where the current intensity remains null until a steep increase is noted at 0,5 V. At this stage the active material is behaving as an anode onto which the oxidation is governed by the Butler-Volmer kinetics until it reaches the anodic current peak of 0,32 V which represents the maximum that the active material is able to oxidize at the given conditions. The once $Co(OH)_2$ covered surface is now fully oxidized into CoOOH as there is no more OH^- required by the active material to react. With the oxidative step completed, the current intensity will decrease until the potential sweep is reversed or until a secondary oxidation is activated by a higher potential. Considering the construction of this system and its limitations, no more reactions will occur during the forward sweep and the electrochemical response will be diffusion controlled. Upon reaching the maximum/ending potential (ψ_{max}) of 0,5 V, the potential sweep is reversed, and the backward step begins. With the potential now decreasing linearly over time under a constant rate of $-\nu$, the Butler-Volmer kinetics govern again and force the active material to be reduced from CoOOH to $Co(OH)_2$. The current decreases to the cathodic current peak of 0,2 V representing the full reduction of the active material. Analogous to the forward sweep, the backward sweep is then controlled by diffusion and increases gradually as the negative current density increases until the potential reaches ψ_{min} again. The simulated CV curve displays a marked faradaic redox behaviour which shape, and values, will be later studied and analysed with the objective of understanding their influence in the overall response of the electrochemical system of cobalt hydroxide. The concentration gradients can also demonstrate the behaviour of the redox species across the diffuse layer throughout time and distance to the active material surface. Some of the key ruling parameters (scan rate, temperature and reaction rate constant) of the simulation will be subject to a sensitivity analysis (Fig. 8) in which they will be varied in defined windows as the electrochemical response of the CV will be observed and conclusions regarding the simulation's approach to reality will be taken. It can be observed that an increasing scan rate results in more positive anodic current peaks and more negative cathodic current peaks, extending the maximum and minimum of the cyclic voltammograms.

This relationship between ν and the current peaks is described by the Randles-Sevcik equation [5] which states that the current peaks are highly dependent on the diffusion properties of the system and of its scan rate.

$$i_p = 2{,}69 \times 10^5 n^{2/3} A D^{1/2} C \nu^{1/2} \quad [5]$$

Randles-Sevcik equation essentially describes that with a higher scan rate the concentration gradient will be higher near the electrode's surface, which abides by the kinetics of Nernst equation. Note that the Nernst equation is not defined in the present simulation setup, but instead, the Butler-Volmer kinetics is. Nernst model is a subset of the Butler-Volmer equation for the particular case of a system in equilibrium which can be mathematically demonstrated as explicitly shown by the work of Kulikovsky et al. [39]. Temperatures of 25, 100, 200, 300 and 400 ºC were imposed in the simulation's parameters and the following sensitivity analysis was conducted. As the temperature increased, the distance between peaks decreased as the CV curves flatten. This behaviour is mathematically expected within the scope of the simulation considering the placement of the temperature term in the Butler-Volmer equations that translate in an Arrhenius-type of exponential response that will always decrease with higher temperatures. In an experimental perspective, it is well reported in literature [40] that the increasing temperature will facilitate the overcoming of the activation energy necessary for the exchange of charged species, reducing the hysteresis of the electrochemical response. This smoothing of the CV curve peaks is noticeable by the less steep current intensity evolution to the peaks, indicating the involvement of more easily achieved energetic states. The heterogeneous reaction rate constant was changed from the initial 0,01 to a final 0,0001 cm/s, and the respective electrochemical behaviour of the CV curve was observed. The variation of the reaction rate constant resulted in interesting curve shapes which can be summarized with the considerable increase of the distance between the oxidation and reduction potentials as the reaction constant decreases. Slower kinetics result in the oxidation requiring higher potentials in order to be achieved, and in reduction requiring more negative potentials, respectively. It can also be observed that as the module of the current peaks decreases, the rate at which they decrease is lower for the same pace of decreasing rate constants. This suggests that the system has a limit to which the kinetics are so slow that the diffusion is then full dominant of its response, requiring a higher potential window as a consequence of lack of kinetic contribution.

The double-layer effect is present in every pseudocapacitor as an effect of the charge separation at the electrode-electrolyte interface. To evaluate the EDLC contribution in the system, an extra step of the simulation was added in which the ideal capacitor approximation. The simulated capacitance proved to be approximately 8 µF which falls in line to the expected capacitance range of EDLC contribution in pseudocapacitors. This contribution is not noticed when added to the full simulation of the cobalt hydroxide system, thus neglected.

A qualitative comparison between the simulated CV curves and curved experimentally obtained for the cobalt hydroxide system was followed Fig. 9. The simulation showcased in Fig. 7 has approximated inputs that were used in the experimentally obtained CV curve of a electrodeposited (by DHBT method) cobalt nanofoam for 45 s and chemically treated with H_2O_2 before being submitted to a CV test in 1 M KOH at 25 ºC and 50 mV s^{-1}.

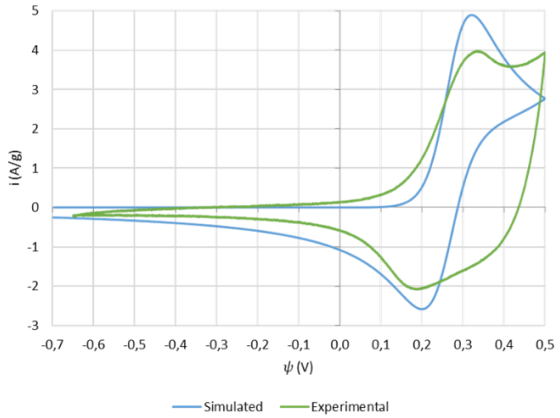

Fig. 9 - Simulated and experimentally obtained CV curves

It is immediately observed that both simulated and experimentally obtained curves share the same potential placement for the cathodic and anodic current peaks at around 0,20 V and 0,32 V, respectively. This suggests that the simulated Butler-Volmer kinetics are a good fit to the real kinetics in nature, respecting the expected $Co(OH)_2$/CoOOH redox potentials. A similar approach to the current peaks is also visible at those potentials, with the distance between peaks being more extensive in the simulated curve than the experimental one. This may have to do with the effectively activated surface of the electrode that participates and enables the redox reactions, usually experimentally obtained through the functionalization methods such as oxidative treatment of

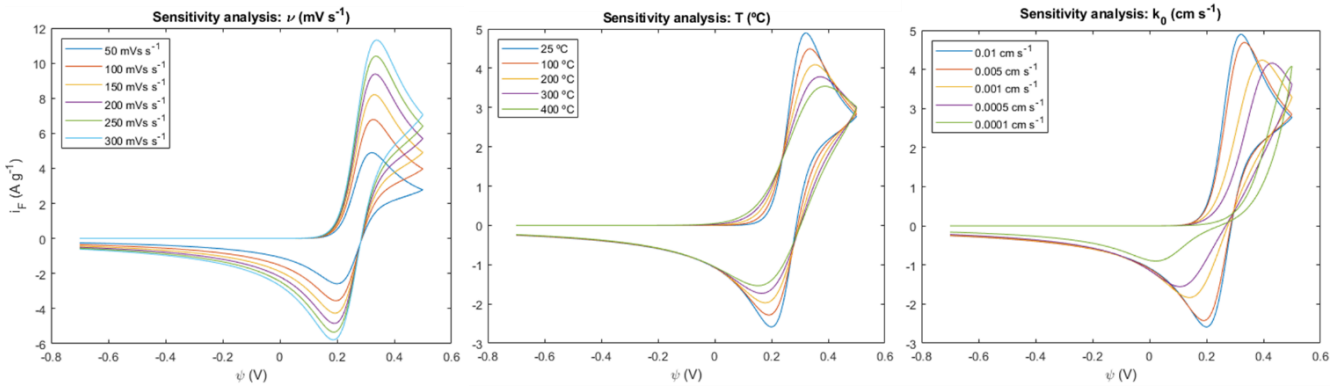

Fig. 8 - Sensitivity analysis to scan rate, temperature, and reaction rate constant, respectively

the metal foam, as described in the previous chapter. Additionally, the overall area of the experimental curve is considerable wider than the simulation most likely as a consequence of other diffusion, and possibly other reactions and kinetic phenomena that are not covered within the simulation model. Unconsidered secondary reactions are also known to occur in these types of pseudocapacitive systems. In fact, the small current peak noticeable at the end of the forward sweep of the experimental curve is possibly related with water electrolysis usually under the form of oxygen evolution reaction (OER). This reaction is essentially the effective oxidation of water under one of possible four mechanisms for alkaline media [41]. Therefore, the addition of the OER was included in the simulation as an extra reaction. According to the Pourbaix diagram of water, for a highly alkaline solution such as the simulations and experiment's case of 1 M (KOH) the standard potential for the oxidation of water is set at ψ_0 of 0,401 V.

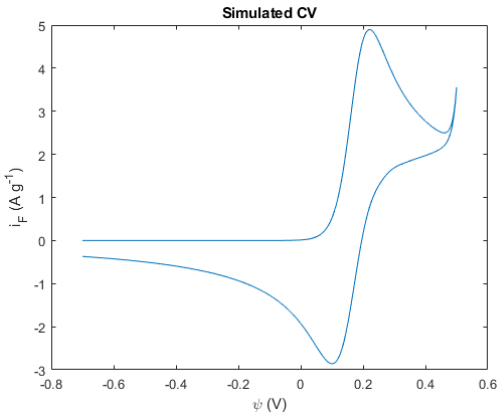

Fig. 10 - Simulated CV with OER

The results present in Fig. 10 showcase the OER occurring at around 0,4 V as expected. The current density would continue to increase until another peak would be established as the limit of the OER. The simulation can thereby include more than one reaction within its kinetics and diffusion models, contributing to a more accurate representation of the reactions that truly occur in the electrode. It is to be noted that the simulated curve is considerably thinner than the experimentally obtained curve. This indicates the presence of other charged species within the electrolyte solution contributing with diffusion phenomena that are usually associated with intercalation mechanisms or other processes. It is difficult to consider the entirety of these processes but not impossible as the simulation's parameters, models and code can be more extensive or simpler depending of the system's complexity. Nevertheless, the cobalt hydroxide nanofoam system can be decently simulated with all the parameters and models previously considered, especially when it comes to pinpoint the placement of the redox current peaks, current density, and potentials.

V. CONCLUSIONS

Pseudocapacitors are promising devices capable of placing a new class of electrochemical capacitors in the gap between electrical capacitors and batteries by providing high power and energy capacities alike, creating solutions for a wide range of applications with their continuous research. Furthermore, understanding the energy storage methods of pseudocapacitors is of utmost importance in the academic scope due to the presence of a wide array of mechanisms that can be practically localised in the functioning of every other electrochemical device. Out of the possible conjugation of pseudocapacitive electrodes, MOHs are clearly the pathway of most interest regarding increasing power and energy densities. Furthermore, among these functionalized metals, cobalt and nickel hydroxide electrode materials pose remarkable electrochemical performances considering their more economic value. The use of these metals in nanoporous frameworks extensively increases the performance with their higher surface areas, which with methods such as DHBT electrodeposition allow the synthesis of complex and highly optimized nanofoam structures in an easy and simple process. By simulating the electrochemical response of a cobalt hydroxide nanofoam approximated system, it has been concluded that the simple mathematical modelling based in the well-known Butler-Volmer kinetics and Fick's laws of diffusion are precise enough to achieve a decent level of accuracy when the pertinent parameters and operating conditions are well defined and adjusted. The simulated CV curves evidenced good accuracy of the current and potential placement of the anodic and cathodic peaks of the system as well as being able to include secondary reactions occurring parallel to the energy storage redox couple such as the OER. The sensitivity analysis of key parameters like scan rate, reaction rate constant, and temperature, demonstrated that the simulation's model abides by the expected behaviour of the CV curve when these parameters are varied.

VI. FUTURE WORK

Future work and research should definitely focus in the optimization of these models towards more accurate reflection of real electrode response by extending to as many processes as are possibly believed and expected to be taking place in an electrochemical cell. Among these processes it is important to highlight the importance of simulating intercalation pseudocapacitance, underpotential deposition, secondary redox reactions (oxidations and reductions occurring inside or outside of the defined potential window) and possible physical and chemical events that influence the diffusion and kinetics of the involved species. To this end, simulation should be focused in understanding the mathematical models that govern these systems and the dominions in which they occur. It is hereby encouraged the use of other discretization methods that simplify and adapt the complex models behind the real processes. Modelling some parameters more thoroughly like the variation of diffusion coefficients with the state of charge is also recommended considering that such treatment will add up to even more accurate simulations.

VII. REFERENCES

1. *IEA, Annual storage deployment, 2013-2018, IEA, Paris https://www.iea.org/data-and-statistics/charts/annual-storage-deployment-2013-2018 (access date: 8/10/2020).*
2. *IEA. (2019) World Energy Investment.*
3. *IEA, Investment in renewable power, a) Renewable power investment, b) Renewable power investment at constant 2018 costs, 2010-2018, IEA, Paris https://www.iea.org/reports/world-energy-investment-2019/power-sector.*
4. *World Energy Council. (2019) Energy Storage Monitor. Latest trends in energy storage 2019 (access date: 8/10/2020).*
5. *Brousse, T., Crosnier, O., Bélanger, D., & Long, J. W. (2017). Capacitive and Pseudocapacitive Electrodes for Electrochemical Capacitors and Hybrid Devices. Metal Oxides in Supercapacitors, 1–24. doi:10.1016/b978-0-12-810464-4.00001-2.*
6. *Jensen, F., Gudla, V. C., Kongstad, I., & Ambat, R. (2019). High frequency pulse anodising of aluminium: Anodising kinetics and optical appearance. Surface and Coatings Technology, 360, 222–*

231. doi:10.1016/j.surfcoat.2018.12.117.
7. *Elabar, D., La Monica, G. R., Santamaria, M., Di Quarto, F., Skeldon, P., & Thompson, G. E. (2017). Anodizing of aluminium and AA 2024-T3 alloy in chromic acid: Effects of sulphate on film growth. Surface and Coatings Technology, 309, 480–489.*
8. *Nickel, D., Dietrich, D., Morgenstern, R., Scharf, I., Podlesak, H., & Lampke, T. (2016). Anodisation of Aluminium Alloys by Micro-Capillary Technique as a Tool for Reliable, Cost-Efficient, and Quick Process Parameter Determination. Advances in Materials.*
9. *Salman, S. A., & Okido, M. (2013). Anodization of magnesium (Mg) alloys to improve corrosion resistance. Corrosion Prevention of Magnesium Alloys, 197–231. doi:10.1533/9780857098962.2.197.*
10. *Song, G.-L., & Shi, Z. (2013). Anodization and corrosion of magnesium (Mg) alloys. Corrosion Prevention of Magnesium Alloys, 232–281. doi:10.1533/9780857098962.2.232.*
11. *Cipriano, A. F., Lin, J., Miller, C., Lin, A., Cortez Alcaraz, M. C., Soria, P., & Liu, H. (2017). Anodization of magnesium for biomedical applications – Processing, characterization, degradation and cytocompatibility. Acta Biomaterialia, 62, 397–417.*
12. *Choi, J., Lim, J. H., Lee, S. C., Chang, J. H., Kim, K. J., & Cho, M. A. (2006). Porous niobium oxide films prepared by anodization in HF/H3PO4. Electrochimica Acta, 51(25), 5502–5507. doi:10.1016/j.electacta.2006.02.024.*
13. *Karlinsey, R. L. (2005). Preparation of self-organized niobium oxide microstructures via potentiostatic anodization. Electrochemistry Communications, 7(12), 1190–1194. doi:10.1016/j.elecom.2005.08.027.*
14. *Kollender, J. P., Mardare, A. I., & Hassel, A. W. (2017). Direct observation of metal dissolution during anodization of niobium. Electrochemistry Communications, 74, 5–8. doi:10.1016/j.elecom.2016.11.011.*
15. *Narayanan, R., & Seshadri, S. K. (2007). Phosphoric acid anodization of Ti–6Al–4V – Structural and corrosion aspects. Corrosion Science, 49(2), 542–558. doi:10.1016/j.corsci.2006.06.021.*
16. *Indira, K., Ningshen, S., Mudali, U. K., & Rajendran, N. (2012). Effect of anodization parameters on the structural morphology of titanium in fluoride containing electrolytes. Materials Characterization, 71, 58–65. doi:10.1016/j.matchar.2012.06.005.*
17. *Delplancke, J.-L., Degrez, M., Fontana, A., & Winand, R. (1982). Self-colour anodizing of titanium. Surface Technology, 16(2), 153–162. doi:10.1016/0376-4583(82)90033-4.*
18. *Simon, P., & Gogotsi, Y. (2008). Materials for electrochemical capacitors. Nature Materials, 7(11), 845–854. doi:10.1038/nmat2297.*
19. *González, A., Goikolea, E., Barrena, J. A., & Mysyk, R. (2016). Review on supercapacitors: Technologies and materials. Renewable and Sustainable Energy Reviews, 58, 1189–1206. doi:10.1016/j.rser.2015.12.249.*
20. *Gudavalli, G. S., & Dhakal, T. P. (2018). Simple Parallel-Plate Capacitors to High–Energy Density Future Supercapacitors. Emerging Materials for Energy Conversion and Storage, 247–301. doi:10.1016/b978-0-12-813794-9.00008-9.*
21. *Stout, D. A., Durmus, N. G., & Webster, T. J. (2013). Synthesis of carbon based nanomaterials for tissue engineering applications. Nanomaterials in Tissue Engineering, 119–157. doi:10.1533/9780857097231.1.119.*
22. *Lee, C., Wei, X., Kysar, J. W., & Hone, J. (2008). Measurement of the Elastic Properties and Intrinsic Strength of Monolayer Graphene. Science, 321(5887), 385–388. doi:10.1126/science.1157996.*
23. *Biesheuvel, P. M., & Dykstra, J. E. (2018). The difference between Faradaic and Nonfaradaic processes in Electrochemistry. arXiv: Chemical Physics.*
24. *C. Niu, G. Han, H. Song, S. Yuan, W. Hou, Intercalation pseudo-capacitance behavior of few-layered molybdenum sulfide in various electrolytes, Journal of Colloid and Interface Science (2019), doi: https://doi.org/10.1016/j.jcis.2019.11.107.*
25. *Thalji, M. R., Ali, G. A. M., Algarni, H., & Chong, K. F. (2019). Al3+ ion intercalation pseudocapacitance study of W18O49 nanostructure. Journal of Power Sources, 438, 227028. doi:10.1016/j.jpowsour.2019.227028.*
26. *Shi, F., Li, L., Wang, X., Gu, C., & Tu, J. (2014). Metal oxide/hydroxide-based materials for supercapacitors. RSC Adv., 4(79), 41910–41921. doi:10.1039/c4ra06136e.*
27. *Singh, A. K., Sarkar, D., Karmakar, K., Mandal, K., & Khan, G. G. (2016).* High-Performance Supercapacitor Electrode Based on Cobalt Oxide–Manganese Dioxide–Nickel Oxide Ternary 1D Hybrid Nanotubes. ACS Applied Materials & Interfaces, 8(32), 20786–20792. doi:10.1021/acsami.6b05933.
28. *Nguyen, T., Montemor, M. de F. (2019). Metal Oxide and Hydroxide-Based Aqueous Supercapacitors: From Charge Storage Mechanisms and Functional Electrode Engineering to Need-Tailored Devices. Advanced Science, 1801797. doi:10.1002/advs.201801797.*
29. *Salunkhe, R. R., Jang, K., Lee, S., & Ahn, H. (2012). Aligned nickel-cobalt hydroxide nanorod arrays for electrochemical pseudocapacitor applications. RSC Advances, 2(8), 3190. doi:10.1039/c2ra01220k.*
30. Huang, L., Chen, D., Ding, Y., Feng, S., Wang, Z. L., & Liu, M. (2013). Nickel–Cobalt Hydroxide Nanosheets Coated on NiCo2O4 Nanowires Grown on Carbon Fiber Paper for High-Performance Pseudocapacitors. Nano Letters, 13(7), 3135–3139. doi:10.1021/nl401086t.
31. Zhang, W., Zhang, X., Tan, Y., Wu, J., Gao, Y., Tang, B., & Wang, Y. (2014). An amorphous nickel–cobalt–boron alloy as advanced pseudocapacitor material. New J. Chem., 38(10), 4666–4669. doi:10.1039/c4nj00912f.
32. Xu, C., Feng, Y., Mao, Z., Zhou, Y., Liu, L., Cheng, W., … Liu, X. (2019). Electronics. doi:10.1007/s10854-019-02313-w, Binary nickel–cobalt metal–organic frameworks as electrode for high performance pseudocapacitor. Journal of Materials Science: Materials in.
33. Vaidyanathan, S., Cherng, J.-Y., Sun, A.-C., & Chen, C.-Y. (2016). Bacteria-Templated NiO Nanoparticles/Microstructure for an Enzymeless Glucose Sensor. International Journal of Molecular Sciences, 17(7), 1104. doi:10.3390/ijms17071104.
34. Sun, H., Zhu, J., Baumann, D., Peng, L., Xu, Y., Shakir, I., et al. (2018). Hierarchical 3D electrodes for electrochemical energy storage. Nature Reviews Materials. doi:10.1038/s41578-018-0069-9.
35. Yu, Z., Tetard, L., Zhai, L., & Thomas, J. (2015). Supercapacitor electrode materials: nanostructures from 0 to 3 dimensions. Energy & Environmental Science, 8(3), 702–730. doi:10.1039/c4ee03229b.
36. Arévalo-Cid, P., Adán-Más, A., Silva, T. M., Rodrigues, J. A., Maçôas, E., Vaz, M. F., & Montemor, M. F. (2020). On the growth and mechanical properties of nanostructured cobalt foams by dynamic hydrogen bubble template electrodeposition. Materials Characterization, 110598. doi:10.1016/j.matchar.2020.110598.
37. Naureen, K. (2019). Production and Functionalization of cobalt nanofoams for energy storage. Instituto Superior Técnico, Universidade de Lisboa.
38. Brown, J. H. (2015). Development and Use of a Cyclic Voltammetry Simulator To Introduce Undergraduate Students to Electrochemical Simulations. Journal of Chemical Education, 92(9), 1490–1496. doi:10.1021/acs.jchemed.5b00225.
39. Kulikovsky, Andrei A. (2019). Analytical Modeling of Fuel Cells || Fuel cell basics. , (), 1–33. doi:10.1016/B978-0-44-464222-6.00008-3.
40. E. M. Gavilán-Arriazu et al 2020 J. Electrochem. Soc. 167 013533.
41. Wang, F, Shifa, T. A., et al., (2015). Recent Advances in transition metal dichalcogenide based nanomaterials for water splitting. Nanoscale, (), 10.1039.C5NR06718A–. doi:10water splitting. Nanoscale, (), doi:10.1039.C5NR06718A.